

- excited states of closed-shell molecules using the constrained-variational approach. *J. Chem. Phys.*, 2009, **131**, 024102.
11. Bag, A., Manohar, P. U. and Pal, S., Analytical dipole moments and dipole polarizabilities of oxygen mono-fluoride and nitrogen dioxide: a constrained variational response to Fock-Space multi-reference coupled-cluster method. *Comput. Lett.*, 2007, **3**, 351(2–4).
 12. Manohar, P. U., Shamasundar, K. R., Bag, A., Vaval, N. and Pal, S., On some aspects of Fock-space multi-reference coupled-cluster singles and doubles energies and optical properties. In *Challenges and Advances in Computational Chemistry and Physics*, 2010, vol. 11, pp. 375–393.
 13. Bag, A., Bhattacharya, S. and Pal, S., Static hyper-polarizability of open shell molecules computed at the FSMRCCSD level using constrained variational approach. In *Recent Advances in Spectroscopy: Theoretical, Astrophysical and Experimental Perspectives* (ed. Chaudhury, R. K. *et al.*), 2010, p. 99–109.
 14. Bag, A., *Linear Response Approach in FSMRCC for Molecular Property*, LAMBERT Academic Publishing, Deutschland, Germany, 2016.
 15. GAMESS, General atomic and molecular electronic structure system. *J. Comput. Chem.*, 1993, **14**, 1347–1363.
 16. Kolos, W. and Wolniewicz, L., Improved theoretical ground-state energy of the hydrogen molecule. *J. Chem. Phys.*, 1968, **49**, 404–410.

ACKNOWLEDGEMENTS. I thank IISER Kolkata for financial support and Dr Pradip Ghorai for permission to publish this work independently. I also thank the reviewer for his valuable comments to improve this article.

Received 10 November 2015; revised accepted 22 July 2017

doi: 10.18520/cs/v113/i12/2325-2328

Satellite-based mapping and monitoring of heavy snowfall in North Western Himalaya and its hydrologic consequences

Bhaskar R. Nikam*, Vaibhav Garg,
Prasun K. Gupta, Praveen K. Thakur,
A. Senthil Kumar, Arpit Chouksey,
S. P. Aggarwal, Pankaj Dhote and
Saurabh Purohit

Indian Institute of Remote Sensing, 4, Kalidas Road,
Dehradun 248 001, India

Snow cover is one of the most important land surface parameters in global water and energy cycle. Large area of North West Himalaya (NWH) receives precipi-

itation mostly in the form of snow. The major share of discharge in rivers of NWH comes from snow and glacier melt. The hydrological models, used to quantify this runoff contribution, use snow-covered area (SCA) along with hydro-meteorological data as essential inputs. In this context, information about SCA is essential for water resource management in NWH region. Regular mapping and monitoring of snow cover by traditional means is difficult due to scarce snow gauges and inaccessible terrain. Remote sensing has proven its capability of mapping and monitoring snow cover and glacier extents in these area, with high spatial and temporal resolution. In this study, 8-day snow cover products from MODIS, and 15-daily snow cover fraction product from AWiFS were used to generate long-term SCA maps (2000–2017) for entire NWH region. Further, the long term variability of 8-daily SCA and its current status has been analysed. The SCA mapped has been validated using AWiFS derived SCA. The analysis of current status (2016–17) of SCA has indicated that the maximum extent of snow cover in NWH region in last 17 years. In 2nd week of February 2017, around 67% of NWH region was snow covered. The comparison of SCA during the 1st week of March and April in 2016–17 against 2015–16 indicates 7.3% and 6.5%, increased SCA in current year. The difference in SCA during 1st week of March 2017 and 1st week of April 2017 was observed to be 14%, which indicates that the 14% SCA has contributed to the snow melt during this period. The change in snow water equivalent retrieved using SCATSAT-1 data also validates this change in snow volume.

Keywords: AWiFS, MOD10A2, North Western Himalaya, snow cover area, SCATSAT-1.

SPATIO-temporal snow cover of North West Himalayas (NWH) river basins has large variations due to difference in topography and hydro-meteorological characteristics of each basin. It is to be noted that heavy snowfall was recorded in many parts of NWH region including the Kashmir Valley during the winter season of 2016–17. According to reports in various national and local agencies and media, unusual variations in temperature and occurrence of high snowfall in early spring season in many parts of NWH broke the last 30-year record¹. The heavy snowfall and persistent positive temperature in early spring season may cause rapid melting of snow and associated hydro-meteorological hazards in lower parts of the river valleys. The recent flood-like situation in the Kashmir valley and occurrence of avalanches in the upper reaches in Kashmir have proven the hazards associated with heavy snowfall. Therefore, the present study was made to map and monitor, current and historical snow cover area (SCA) in NWH region.

Regular mapping and monitoring of seasonal snow cover by traditional ground-based methods is difficult due to scanty snow gauges, inaccessible terrain during

*For correspondence. (e-mail: bhaskarnikam@iirs.gov.in)

peak winters, rugged and high altitude topography and remoteness of the mountains. Space-based remote sensing has already proved its capability of mapping and monitoring SCA with high temporal and spatial resolution^{2,3}. One of the most commonly used methods for operational and research oriented snow cover mapping using optical remote sensing is Normalized Difference Snow Index (NDSI) which is the normalized ratio of difference and addition of reflectance in green and shortwave infrared bands^{1,4-7}. Snow is normally assumed to be present if the NDSI exceeds a value of 0.4. Recent studies have shown that the optimum value of the threshold varies seasonally⁸. Similarly, the presence of forest cover, cloud cover, and water bodies in the region may cause errors in SCA estimation, if only NDSI is used for SCA mapping. To overcome these limitations, a rule-based algorithm was proposed and implemented⁹⁻¹¹ for operational mapping of SCA using moderate-resolution imaging spectroradiometer (MODIS) sensor on-board Terra and Aqua satellites, which provide daily, 8-daily and 16-daily SCA products from the year 2000 onwards. The 8-day maximum snow cover data from MODIS 8-day snow cover product (MOD10A2, NSIDC)¹² with spatial resolution of 500 m was used in this study to map and monitor SCA for the period from 2000 to 2017. In the present analysis, a weekly maximum snow cover of winter season, starting from Julian day 313 (1 November) to Julian day 89 (30 March) was analysed using automated SCA extraction tool developed in-house and standard geospatial tools.

One tile of MOD10A2 consists of 2400 by 2400 rows and columns with 500 m pixel resolution and is available in sinusoidal map projection. These datasets are usually coded according to each land cover, e.g. the snow covered area is represented by the code 200, lake ice by 100, cloud by 50, etc.¹³. As the pixel value for the snow-covered pixels is constant, the process of extraction of SCA can be easily automated. The process of snow cover mapping becomes difficult in the case of existence of cloud over the snow-covered areas for longer duration (week or more). In such cases, the area will be coded as cloud mask (code: 50) in MOD10A2; the underlying areas may however still be covered with snow. Manual rectification of snow under cloud is difficult due to the dependence on available geo-statistical tools in GIS software. To overcome this problem, an automated snow cover mapping tool was developed and used in the present study. The tool initially generated a permanent snow cover map based on frequency analysis of the pixel as snow, considering all the long-term snow cover datasets available. In the second run, the tool analysed three subsequent time period snow cover products ($t-1$, t , $t+1$; where t is the current time period). The pixel in the input dataset of time period t designated by code 200 was marked as snow pixel and other ambiguous pixels with cloud cover (code 50) were analysed with reference to

permanent snow cover map generated in the first step and snow cover products of previous ($t-1$) and subsequent time period ($t+1$) (ref. 14). Elevation mask of 1500 m was used in the tool to avoid misclassification of pixels below 1500 m elevation into snow cover area^{15,16}. SCA products generated using IRS Resourcesat 1 and 2 AWiFS data are available on ISRO's Geoportals, Bhuvan (<https://bhuvan.nrsc.gov.in>). These products were used to validate the accuracy of SCA mapped using MOD10A2 data. The SCA derived from AWiFS products and MOD10A2 products for the period January 2017 to March 2017 were compared and 0.9 coefficient of determination was achieved in this comparison. Per cent error in SCA mapping using MODIS products in reference to AWiFS derived SCA was in the order of 7–14%. The variation in SCA statistics in these two products may be attributed to difference in spatial and temporal resolution of these products. In the present study, MOD10A2 was preferred over AWiFS derived SCA fraction product due to its long-term data availability, higher spatial and temporal resolution.

The sub-basin wise temporal SCA was derived using histogram extraction tool developed in-house using Interactive Data Language. The sub-basin boundaries of NWH region have been taken from India Water Resources Information System demarcated by Central Water Commission (CWC), as shown in Figure 1. SCA was reported in terms of fractional area (SCA/basin area) for better representation and discussed at weekly time scale. Long-term SCA was analysed and mean (SCA_{mean}), maximum (SCA_{max}) and minimum SCA (SCA_{min}) of each time step for respective sub-basin was identified. The temporal variation in fractional SCA during winter season of 2016–17 and the long-term trend of SCA_{mean} of the entire NWH is represented in Figure 2. Figure 1 corresponds to maximum SCA (around 67%) in the winter of 2016–17 which occurred during the second week of February 2017. It is also evident from Figure 2 that fractional SCA is highest (around 0.67) during the same period. The temporal identifiers a, b, c in Figure 2 represents the fractional SCA for the corresponding time steps mentioned in Figure 3 a–c. It is also to be noted that SCA in entire NWH was consistently higher than long-term mean SCA since first week of January 2017.

The SCA of each time step of winter season 2016–17 was compared with long-term SCA_{mean}, SCA_{max}, SCA_{min} (2000–01 to 2015–16) for the respective sub-basins (the SCA plots are available at: <https://iirs.gov.in/content/sca-mapping-activity>). The comparison between SCA of winter season of 2015–16 and 2016–17, given in Table 1, indicates significant increase in SCA during the later period in most sub-basins. The SCA_{max} in winter season of 2016–17 was identified for each sub-basin along with its week of occurrence. The SCA on same dates in the previous winter season were used to highlight the difference in SCA during winter season of 2016–17 (Table 1). The

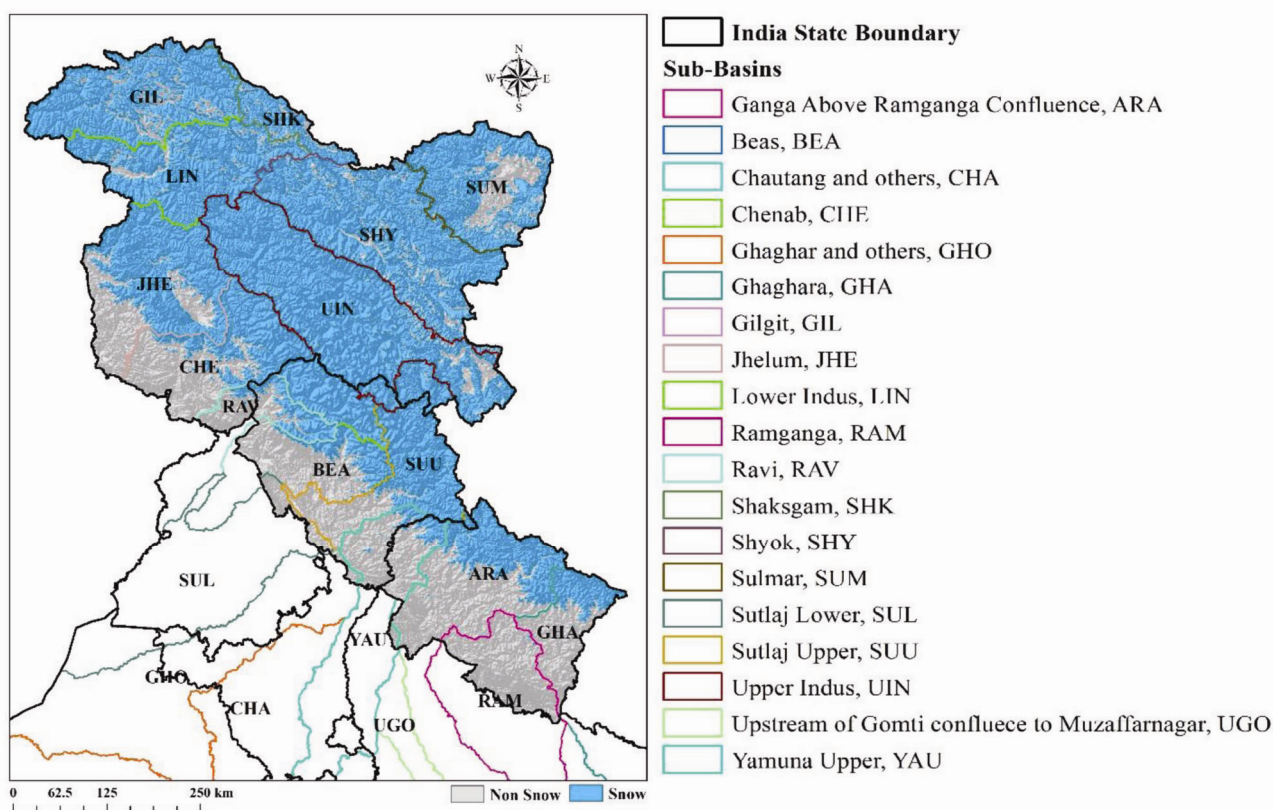


Figure 1. Eight-day maximum SCA in 2nd week of February 2017 derived from MOD10A2 product.

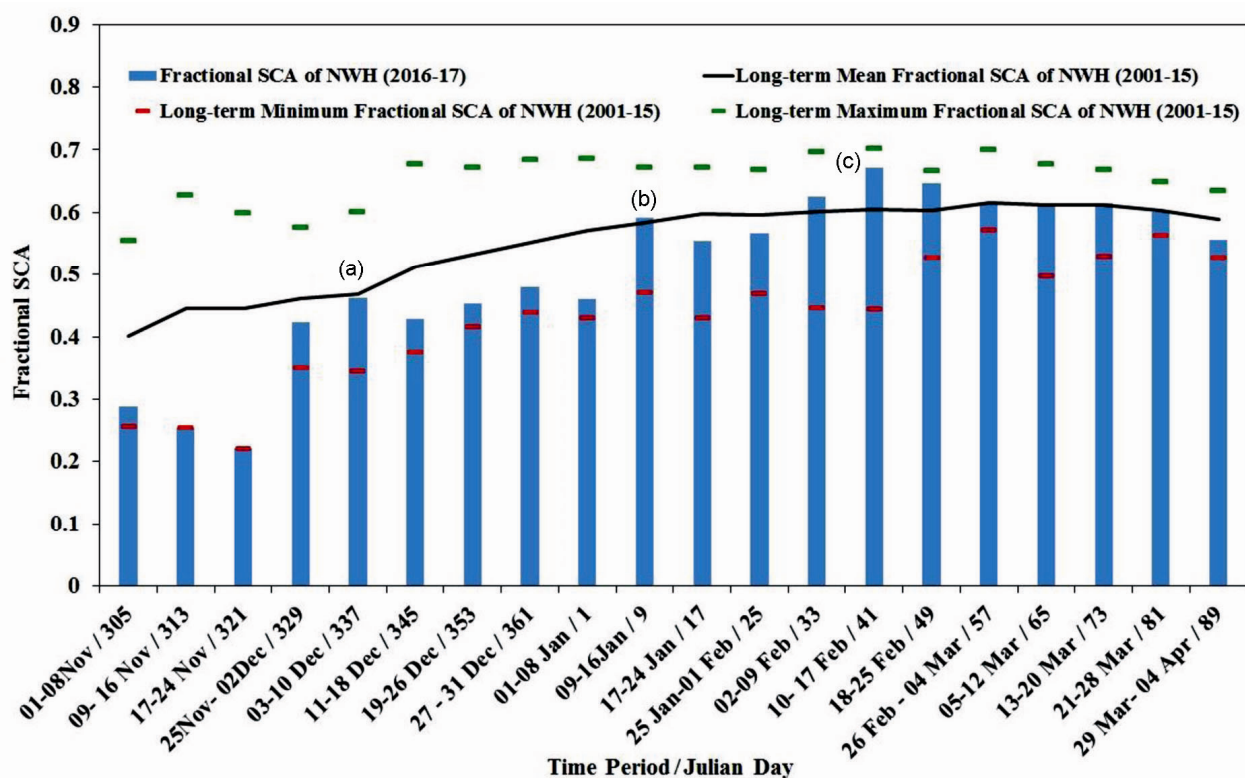


Figure 2. Comparison of fractional snow cover in NWH.

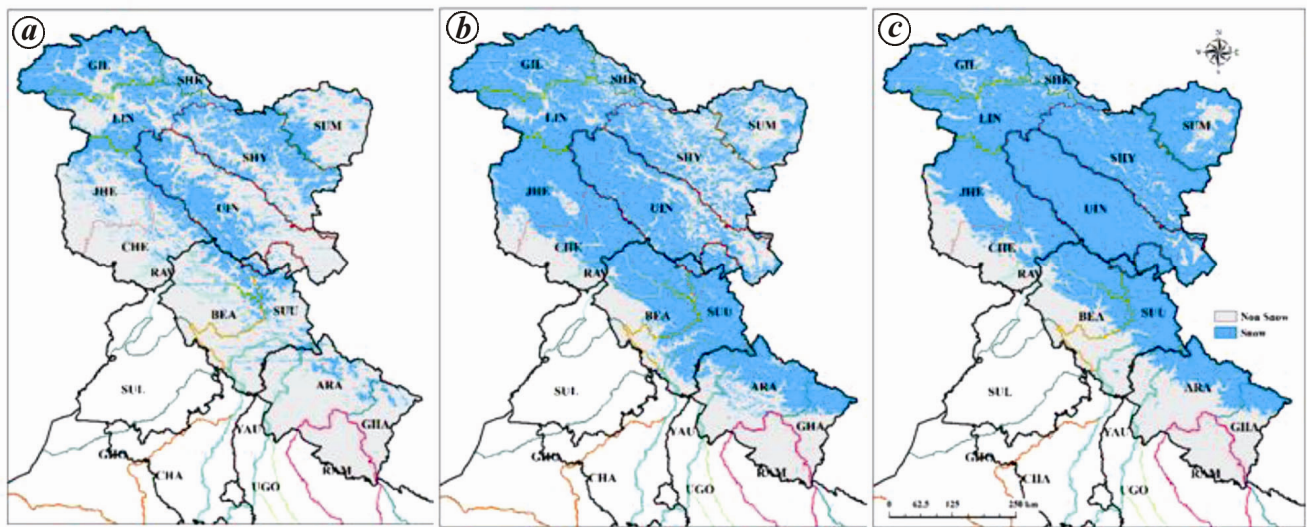


Figure 3. Temporal change in SCA during winter 2016–17. *a*, 25 November–2 December 2016; *b*, 9–16 January 2017; *c*, 10–17 February 2017.

Table 1. Basin-wise analysis of SCA in NWH

Basin name	Date of SCA _{max}	SCA _{max} fraction	SCA on same date in 2015–16	SCA status in first week of March in year			SCA status in first week of April in year		
				2016	2017	Change (%)	2016	2017	Change (%)
ARA	09–01–17	0.30	0.24	0.23	0.25	2.20	0.22	0.24	1.57
Beas	09–01–17	0.34	0.25	0.19	0.21	1.50	0.15	0.19	3.83
Chenab	09–01–17	0.67	0.59	0.52	0.61	9.50	0.52	0.54	2.77
Gilgit	18–02–17	0.84	0.73	0.73	0.83	9.50	0.74	0.71	–2.86
Jhelum	09–01–17	0.76	0.53	0.44	0.54	10.10	0.39	0.39	0.87
Lower Indus	10–02–17	0.88	0.70	0.72	0.79	7.20	0.65	0.62	–2.97
Ravi	17–01–17	0.38	0.26	0.20	0.27	7.10	0.18	0.22	4.17
Shaksgam	18–02–17	0.76	0.66	0.71	0.69	–2.30	0.84	0.85	0.95
Shyok	10–02–17	0.85	0.54	0.66	0.70	3.90	0.59	0.82	23.60
Sulmar	10–02–17	0.74	0.18	0.23	0.47	23.60	0.22	0.42	20.17
Sutlaj Upper	10–02–17	0.74	0.66	0.65	0.70	5.70	0.56	0.67	11.22
Upper Indus	10–02–17	0.95	0.65	0.69	0.85	16.30	0.61	0.81	20.87
Yamuna Upper	09–01–17	0.16	0.07	0.05	0.06	0.50	0.04	0.05	1.07
Average						7.29			6.56

maximum SCA observed for the year 2017 in all the sub-basins was approximately 10–50% higher when compared to SCA of the same time period in 2016. At NWH scale, 20% increase in SCA during winter season of 2016–17 was observed, especially in the months of January to April 2017 when compared to previous year. Additionally, to analyse the status of SCA in spring season of 2017, the comparison of fractional SCA between the first week of March and April (2016 and 2017) was also carried out (Table 1). The average increase of 7.29% and 6.56% (approx.) was observed in SCA during the first week of March and April 2017 respectively, when compared to 2016.

The temporal increase in SCA of NWH region from November 2016 to February 2017 is visualized in the representative SCA maps shown in Figure 3. The basin-wise

analysis of SCA during winter season of 2016–17 revealed that, the SCA_{max} values in Upper Ganga, Beas, Chenab and Jhelum sub-basins occurred during the second week of January and it varied from 0.3 to 0.76 (Table 1 and Figure 3 *b*). However, in Upper Sutlaj, Lower Indus, Shyok, Sulmar sub-basins SCA_{max} was observed in the second week of February 2017, ranging from 0.73 to 0.95 (Table 1 and Figure 3 *c*). However, the SCA_{max} in Gilgit and Shaksgam sub-basins was noticed in the third week of February 2017, with value varying from 0.75 to 0.84 (Table 1). Further, to validate the increase in snowfall/snow cover, observed data from field instrument (Snow Pack Analyser) installed by IIRS at Dhundi, Manali (falls in Upper Beas Sub-basin) for measuring snow properties, was analysed. Figure 4 shows significant increase in snow depth (1–1.5 m) during first week of

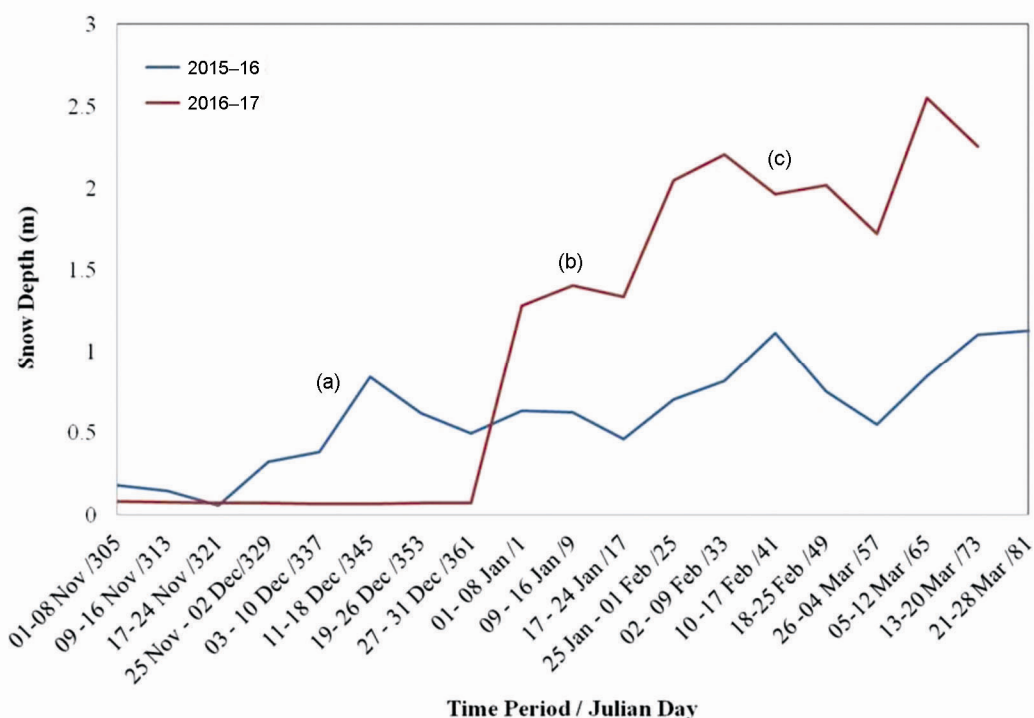


Figure 4. Observed snow depths at Dhundi, Manali (Upper Beas sub-basin).

Table 2. Observed rainfall (mm) and temperature (°C) data of few IMD-AWS in Jhelum Basin

Station name/date	3 April 2017	4 April 2017	5 April 2017	6 April 2017	7 April 17	8 April 2017	9 April 2017
Srinagar	Rainfall	0	29	4	3	2	2
	Avg. temp.	14.3	9.14	8.78	2.63	6.21	7.7
Pahalgam	Rainfall	1	46	21	33	19	11
	Avg. temp.	6.2	6.31	6.4	0.5	2.25	2.71
Rambagh	Rainfall	0	27	67	27	27	3
	Avg. temp.	16	9.38	8.93	2.15	6.19	7.84

December 2016 (Figure 3 a), first week of January 2017 (Figure 3 b) and second week of February 2017 (Figure 3 c) when compared to the previous year; resulting in significant increase in SCA of NWH region in subsequent weeks as observed in SCA results. Similar trend was observed during the first week of March 2017.

It is to be noted that maximum snow cover of Jhelum basin in the first week of March 2017 was 10% higher than the same period of 2016. However, the first week of April SCA was similar in both the years (Table 1). Further analysis showed that 14% more area contributed to snow melt runoff in the basin from the first week of March to the first week of April 2017. The same trend was observed in Gilgit and Chenab river sub-basins. Recently, the Indian Space Research Organisation launched new microwave satellite SCATSAT-1 which is a K_u band scatterometer (ISRO)¹⁷.

As K_u band has the highest sensitivity to snow, daily gridded data from SCATSAT-1 at 2.25 km resolution was used to compute change in snow water equivalent

(Δ SWE) for NWH using one layer Radiative Transfer Model¹⁸. SWE derived from SCATSAT-1 data are preliminary results based on backscatter change between two dates and calibrated using SWE change as observed on ground. The backscatter of the 1st and 2nd week of January 2017 is shown in Figure 5 a and b. Ground observed SWE data was available for one station (i.e. Dhundi, Manali) and the relation between Δ SWE from SCATSAT with observed data is shown in Figure 5 d. The calibrated relation was then used to quantify changes in SWE in other river basins in NWH (as shown in Figure 5 c). It was analysed that SWE decreased by 37 mm from the first week of March to the first week of April 2017 in Jhelum River sub-basin which is in concurrence with 14% decrease in SCA during the same time period.

Heavy snowfall in NWH, leading to higher SCA in spring season, increases the probability of flash floods, landslide, sudden increase in river flow and associated hazards in the region, along with positive impacts such as increase in hydropower generation and reservoir storage.

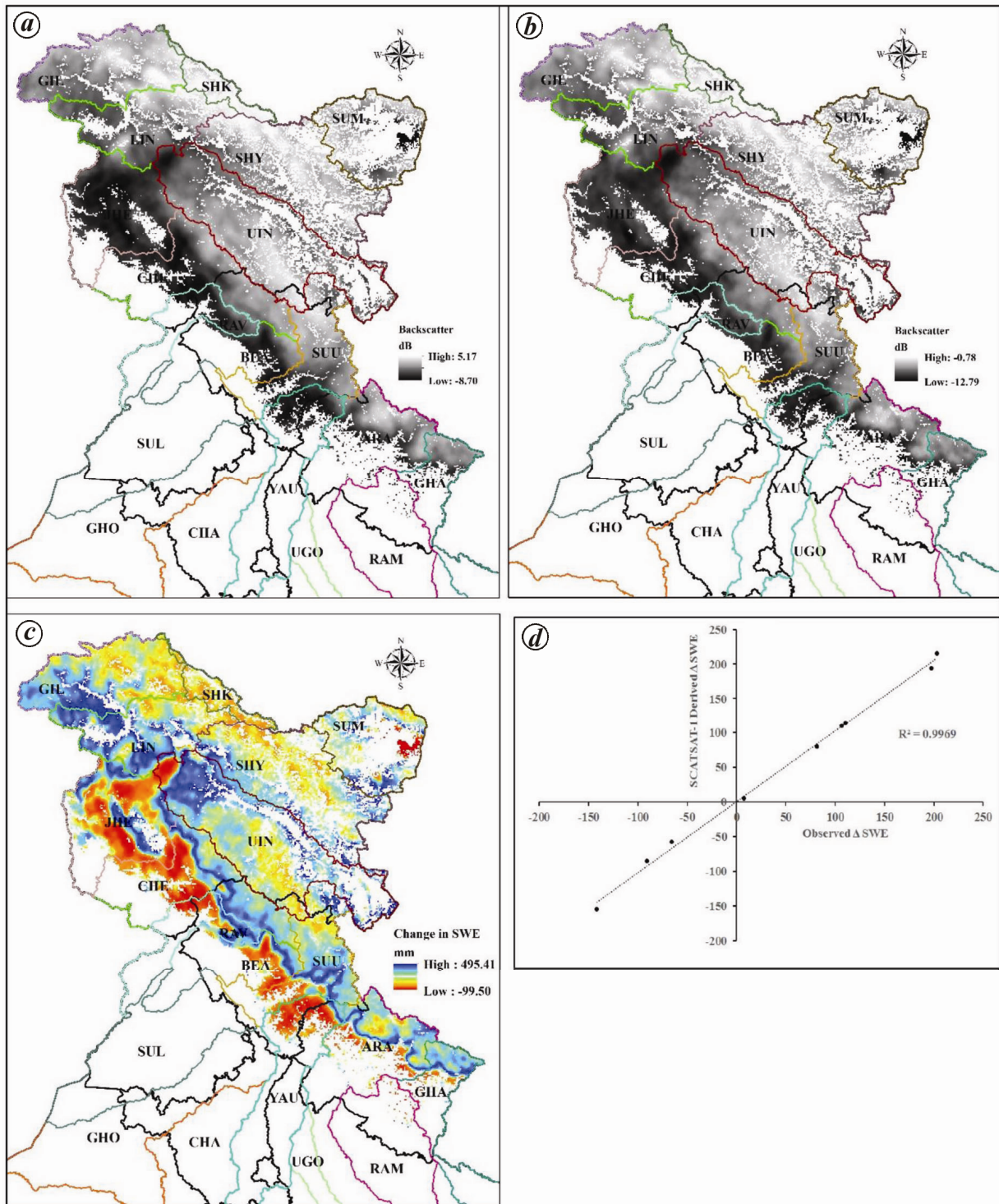


Figure 5. *a*, Backscatter 1st week January 2017; *b*, Backscatter 2nd week January 2017; *c*, Change (Δ) in SWE Derived from SCATSAT-1; *d*, Relationship between observed and SCATSAT-1 derived Δ SWE at Dhundi, Manali.

The increased SCA, snow depth may produce higher snow melt/discharge during upcoming spring and summer seasons in these sub-basins. The early spring floods in Kashmir Valley and multiple avalanches in higher reaches are few examples of this kind of snow hazards. It

was realized that the main cause of these hazards are heavy snowfall in the region, followed by precipitation in early April. The unexpected continuous rains in the first week of April 2017 (Table 2) and snow melt would have increased the volume of discharge, which can surpass the

danger flood level in lower parts of Jhelum valley. According to the India Meteorological Department (IMD) Automatic Weather Station (AWS) data, some of the sites which are located in Jhelum river basin received good spring rainfall during 4–8 April 2017. During this time, temperature was consistently on higher side, except for 6 April 2017 (IMD)¹. This rainfall during early spring causes rapid melting of accumulated winter snow due to positive energy feedback from rain on the snow process. The accelerated snow melt and surface runoff generated from excess rainfall increases the risk of flood in the sub-basin.

This was validated with CWC forecast and observation data showed peak flood water level at Rammunsibagh gauging site near Srinagar town at 1586.8 m on 7 April 2017, 1100 hrs. This flood peak remained above danger level of 1586.45 m till 8 April 2017, 0100 hrs. Further flood level gradually decreased to 1585.1 m on 9 April 2017 at 0600 hrs which is below the warning level of 1585.5 m (CWC)¹⁹. In addition to the flood situation in lower parts of Jhelum River, few cases of snow avalanches were also reported in January and April 2017 in Jammu and Kashmir. On 6 April 2017, snow avalanche in Batalik sector of Ladakh was reported, as heavy snowfall of 83.9 mm was recorded on 5 April 2017. Thus, mapping and monitoring of SCA along with its use in weather and hydrological forecast becomes important from a hydro-meteorological hazard as well as an overall water resources management point of view. IIRS has initiated a new research proposal where short, medium and long-term hydrological forecast will be done for major river basins of NWH to address such events based on scientific studies. Additionally, Synthetic Aperture Radar (SAR) data can provide SCA especially during wet snow time^{20,21}. Therefore, SAR data from RISAT-1 and Sentinel-1, 2 can be used to map SCA in areas affected by persistent cloud cover and during melt season. Change in albedo of snow cover also affects the rate of snow melt; hence change in albedo of SCA must also be considered in the assessment of snow melt.

1. IMD, India Meteorological Department: AWS Lab Pune; <http://www.imdaws.com/ViewAwsData.aspx> (accessed on 10 April 2017).
2. Aggarwal, S. P., Thakur, P. K., Nikam, B. R. and Garg, V., Integrated approach for snowmelt run-off estimation using temperature index model, remote sensing and GIS. *Curr. Sci.*, 2014, **106**(3), 397–407.
3. Kulkarni, A. V., Singh, S. K., Mathur, P. and Mishra, V. D., Algorithm to monitor snow cover using AWiFS data of Resourcesat-1 for the Himalayan region. *Int. J. Remote Sens.*, 2006, **27**, 2449–2457.
4. Dozier, J., Snow reflectance from Landsat-4 thematic mapper. *IEEE Trans. Geosci. Remote Sens.*, 1984, **22**, 323–328.
5. Dozier, J. and Marks, D., Snow mapping and classification from Landsat Thematic Mapper (TM) data. *Ann. Glaciol.*, 1987, **9**, 97–103.
6. Dozier, J., Spectral signature of alpine snow covers from the Landsat thematic mapper. *Remote Sens. Environ.*, 1989, **28**, 9–22.
7. Dozier, J. and Frew, J., Computational provenance in hydrologic science: a snow mapping example. *Philos. Trans. R. Soc. London, Ser. A.*, 2009, **367**, 1021–1033.
8. Vogel, S. W., Usage of high-resolution Landsat-7 band-8 for single band snow cover classification. *Ann. Glaciol.*, 2002, **34**, 53–57.
9. Dorothy, K. H. *et al.*, Algorithm Theoretical Basis Document (ATBD) for the MODIS Snow and Sea Ice-Mapping Algorithms, NASA Goddard Space Flight Center, Greenbelt, Maryland, 2001; <https://modis-snow-ice.gsfc.nasa.gov> (accessed on 13 February 2017).
10. Hall, D. K., Riggs, G. A., Salomonson, V. V., DiGirolamo, N. E. and Bayr, K. J., MODIS snow cover products. *Remote Sens. Environ.*, 2002, **83**, 181–194.
11. Hall, D. K., Riggs, G. A. and Román, M. O., VIIRS Snow Cover Algorithm Theoretical Basis Document (ATBD), Version 1.0, NASA Goddard Space Flight Center, Greenbelt, Maryland, 2015, p. 38.
12. NSIDC, National Snow and Ice Data Centre website: Snow Cover Products; <https://nsidc.org/data/MOD10A2> (accessed on 13 February 2017).
13. Hall, D. K. and Riggs, G. A., MODIS/Terra Snow Cover 8-Day L3 Global 500 m Grid, Version 6. Boulder, Colorado USA. NASA National Snow and Ice Data Center Distributed Active Archive Center, 2016; doi: <http://dx.doi.org/10.5067/MODIS/MOD-10A2.006> (accessed on 13 February 2017).
14. Nikam, B. R., Garg, V., Gupta, P. K., Thakur, P. K., Aggarwal, S. P. and Kumar, A. S., A Preliminary Assessment Report on Assessment of Long-Term and Current Status (2016-17) of Snow Cover Area in North Western Himalayan River Basins using Remote Sensing. Technical Report, IIRS/WRD/Technical Report/2017/212, IIRS Dehradun, 2017, p. 26.
15. Jain, S. K., Goswami, A. and Saraf, A. K., Accuracy assessment of MODIS, NOAA and IRS data in snow cover mapping under Himalayan conditions. *Int. J. Remote Sens.*, 2008, **29**(20), 5863–5878.
16. Sharma, V., Mishra, V. D. and Joshi, P. K., Topographic controls on spatio-temporal snow cover distribution in Northwest Himalaya. *Int. J. Remote Sens.*, 2014, **35**(9), 3036–3056.
17. ISRO, Indian Space Research Organisation; <http://www.isro.gov.in/Spacecraft/scatsat-1> (accessed on 10 April 2017).
18. Yueh, S., Cline, D. and Elder, K., POLSCAT Ku-band Radar Remote Sensing of Terrestrial Snow Cover. IEEE Proc. International Geoscience and Remote Sensing Symposium-2008, Boston, MA, USA, 7–11 July 2008 (doi:10.1109/IGARSS.2008.4779276).
19. CWC, Central Water Commission: Flood Forecast Portal; <http://www.india-water.gov.in/ffs/hydrograph/> (accessed on 10 April 2017).
20. Thakur, P. K., Aggarwal, S. P., Arun, G., Sood, S., Kumar, A. S., Snehmani and Dobhal, D. P., Estimation of snow cover area, snow physical properties and glacier classification in parts of Western Himalayas using C-band SAR data. *J. Indian Soc. Remote Sens.*, 2016; doi:10.1007/s12524-016-0609-y.
21. Thakur, P. K., Garg, P. K., Aggarwal, S. P., Garg, R. D. and Snehmani, Snow cover area mapping using synthetic aperture radar in Manali watershed of Beas River in the Northwest Himalayas. *J. Indian Soc. Remote Sens.*, 2013; doi:10.1007/s12524-012-0236-1.

Received 11 April 2017; revised accepted 3 August 2017

doi: 10.18520/cs/v113/i12/2328-2334